Inert Filler Selection Strategies in Li-ion Gel Polymer Electrolytes

Jun Pan,[†] *Pei Zhao,*[§] *Heliang Yao,* [§] *Lulu Hu,*[§] *and Hong Jin Fan**[†]

[†]School of Physical and Mathematical Sciences, Nanyang Technological University, Singapore 637371, Singapore.

[§]State Key Laboratory of High-Performance Ceramics and Superfine Microstructure, Shanghai Institute of Ceramics, Chinese Academy of Science, Shanghai 200050, China.

ABSTRACT: The main role of inert fillers in polymer electrolytes is to enhance ionic conductivity. However, lithium ions in gel polymer electrolytes (GPE) conduct in the liquid solvent rather than along the polymer chains. So far, the main role of inert fillers in improving the electrochemical performance of GPE is still unclear. Here, various low-cost and common inert fillers (Al_2O_3, SiO_2, TiO_2, ZrO_2) are introduced into GPEs to study their effects on Li-ion polymer batteries. It is found that the addition of inert fillers has different effects on ionic conductivity, mechanical strength, thermal stability, and dominantly, interfacial properties. Compared with other gel electrolytes containing SiO_2, TiO_2, or ZrO_2 fillers, the one with Al_2O_3 fillers exhibit the most favorable performance. The high performance is ascribed to the interaction between the surface functional groups of Al_2O_3 and $LiNi_{0.8}Co_{0.1}Mn_{0.1}O_2$ which alleviates the decomposition of the organic solvent by the cathode, resulting in the formation of a high-quality Li^+ conductor interfacial layer. This study provides an important reference for the selection of fillers in GPEs, surface modification of separators, and cathode surface coating.

KEYWORDS: Inert fillers, Gel polymer electrolytes, Li^+ conductive interface layer, Intermolecular interaction, Lithium-ion batteries

1. INTRODUCTION

As a successfully commercialized secondary battery for energy storage, lithium-ion batteries (LIBs) with both high energy density and long cycle life are widely used in portable and power devices.[1-3] Solid electrolytes are regarded as the solution to the problem of organic liquid electrolyte leakage. Compared with inorganic solid electrolytes with poor interfacial contact, polymer solid electrolytes have the potential for large-scale production due to their flexibility and enhanced interfacial contact. But polymer solid electrolytes are limited by their low ionic conductivity.[4-6] Currently, gel polymer electrolytes (GPEs), which combine the advantages of liquid electrolytes and polymer electrolytes to achieve high ionic conductivity and flexibility, have attracted widespread attention.[7,8]

Fillers including lithium-ion conductor ($Li_7La_3Zr_2O_{12}$, $Li_2Al_{0.5}Ti_{0.5}(PO_4)_3$, $Li_{10}GeP_2S_{12}$) and inert fillers (Al_2O_3, SiO_2, TiO_2, ZrO_2) have been widely used in polymer electrolytes.[9-18] Among them, inexpensive and air-stable inert fillers hold promise for industry applications. It has been recognized that the improvement in the polymer battery performance after adding inert fillers is mainly due to the increase in ionic conductivity.[19-21] However, the conduction of lithium ions in GPE is thought to be similar to that in conventional liquid electrolytes rather than along the polymer chains. The ionic conductivity of GPEs can be increased if a mesoporous inert filler that confines more liquid is added.[22,23] Inert fillers may bring in the following effects. 1) The added inert fillers form a three-dimensional network electrolyte to enhance the mechanical strength of the electrolyte membrane.[24,25] 2) The uniform dispersion of inert fillers can act as a rigid framework, preventing the rapid conduction of heat into the matrix, and thereby alleviating thermal degradation.[26,27] 3) The functional inert fillers generate a Li^+ conductor interface layer through the in-situ reaction at the electrode-electrolyte interface, which reduces the interface

impedance.[28,29] However, it is still unclear what are the main factors that determine the battery performance. A systematic investigation on the above properties of inert fillers in GPEs, which has been lacking, will help guide the filler selection.

Herein, we synthesized a GPE by using poly(vinylidene fluoride)-co-hexafluoropropylene (PVDF-HFP), Lithium bis(trifluoromethane sulfonyl)imide (LiTFSI), and propylene carbonate (PC). Different fillers, including p-block (Al_2O_3, SiO_2) and d-block (TiO_2, ZrO_2) oxide, are added and tested for mechanical strength, thermal stability, ionic conductivity, and interfacial impedance. It is found that the GPE containing Al_2O_3 performs better than the GPE containing SiO_2, TiO_2, and ZrO_2. The reaction is that there is an interaction between $LiNi_{0.8}Co_{0.1}Mn_{0.1}O_2$ (NCM811) and the functional groups in Al_2O_3 filler, which alleviates the decomposition of the organic solvent by the cathode and thus benefits the formation of interfacial films of low-resistance lithium-ion conductors. This interpretation is confirmed by electrochemical impedance spectroscopy (EIS), Fourier transform infrared spectroscopy (FTIR), and X-ray photoelectron spectroscopy (XPS) for interfacial film analysis. This work highlights the importance of interface design between fillers and electrodes, and may guide the selection of functional fillers according to different cathode materials.

2. EXPERIMENTAL SECTION

Materials. All the chemicals were purchased and used directly without further purification. NCM811, $LiCoO_2$, and $LiPePO_4$ were purchased from Binbin Co., Ltd., Al_2O_3, SiO_2, TiO_2, and ZrO_2 (50 nm) were purchased from Macklin. PC (99.7%), LiTFSI (99%), and PVDF-HFP (Mw~400,000) were purchased from Aladdin. Acetone (99.5%) was purchased from Sinopharm, Li sheet was purchased from China Energy Lithium Industry.

Electrolyte preparation. PVDF-HFP (0.5 g), LiTFSI (0.24 g), PC (0, 0.25, 0.5 and 0.75 mL) and 0.025, 0.05, 0.075, 0.1 g inert fillers (Al_2O_3, SiO_2, TiO_2, and ZrO_2) were dissolved in acetone (5 mL) under continuous stirring for 3 h at 50 °C and then cooled at 25 °C to obtain a homogeneous electrolyte slurry. Next, the electrolyte slurry was coated on the centrifugal membrane with a doctor blade and dried at 60 °C for 1 h to obtain a 100 μm film. Finally, the electrolyte film was punched into a disc with a diameter of 19 mm.

Structure Characterization. Scanning electron microscope (SEM) images were obtained by HITACHI S4800 Field-emission scanning electron microscope (Japan). Transmission electron microscope (TEM) images were obtained using an aberration-corrected FEI Tecnai F20 transmission electron microscope (USA). The chemical valence and composition analysis were determined on a Thermo Scientific X-ray photoelectron spectrometer (XPS, ESCALAB 250, USA). FTIR spectra were conducted on a Bruker Tensor 27 infrared spectrum analyzer. Thermal gravimetric analysis (TGA) was gained on a thermal analyzer (Mettler Toledo TGA/SDTA85, Canada) from room temperature to 800 °C filled with N_2. X-ray diffraction (XRD) patterns measured were on a Bruker D8 Adv. powder diffractometer (Cu kα radiation, λ=1.5418 Å, Germany). Tensile tests were carried out on a universal testing machine (Instron-5566, USA).

Electrochemical measurements. Electrochemical measurements were examined in CR2032-type coin cells. NCM811 (or $LiCoO_2$, $LiPePO_4$), PVDF, and acetylene black were mixed in a weight ratio of 8:1:1, and nitrogen methyl pyrrolidone was used as a solvent to make cathode slurries. The slurry was spread on Al foil with a spatula and then dried in a vacuum at 100 °C for 6 h. The foils were then punched into 12 mm discs with an active material mass loading of 2.0-2.5 mg cm^{-2}. Then, gel polymer lithium-ion batteries were assembled in an Ar-filled glove box (MB-Labstar, 1200/780, $H_2O < 0.5$ ppm; $O_2 < 0.5$ ppm) with Li metal as counter

electrode and the GPEs as electrolytes. Galvanostatic discharge/charge was obtained on a battery cycler (LAND CT-2001A, China) at 25 °C with battery operating voltages of 3-4.2 V for NCM811//Li, 3-4.2 V for $LiCoO_2$//Li, and 2.5-3.8 V for $LiPePO_4$//Li. EIS spectra were accomplished on an Autolab PGSTAT 302N electrochemical workstation (Switzerland) from 100 kHz to 0.01 Hz. The Li^+ conductivity was examined at 25 °C using symmetric SS|GPEs|SS (SS = stainless steel). Linear sweep voltammetry (LSV) was carried out at 25 °C using Li|GPEs|SS coin cells.

3. RESULTS AND DISCUSSION

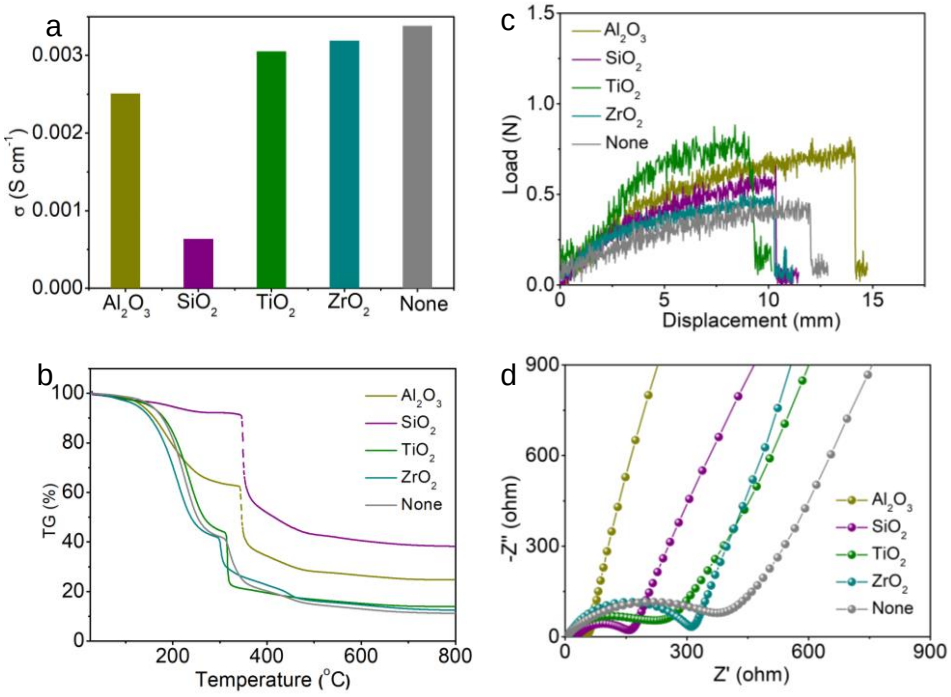

Figure 1. Physical and chemical properties of GPEs with different inert fillers. (a) The ionic conductivity. (b) TGA curves. (c) Tensile strength. (d) EIS spectra for NCM811//GPEs//Li.

Physical and chemical properties of GPEs. High dielectric constant and air-stable PVDF-HFP is chosen as the polymer substrate.[30] LiTFSI, which has high electrical conductivity and electrochemical stability, is used as the lithium salt.[31] To determine the optimum ratio of fillers, different contents (0%, 5%, 10%, 15%, 20%) of silica are used as examples (LiTFSI-PVDF-HFP-SiO_2). XRD patterns show that the crystallinity of the polymer decreases with the increase of the amount of SiO_2, indicating that the filler affects the structure of the polymer chain.[32] When the proportion of filler reaches 15% (0.075 g), the ionic conductivity reaches the maximum. A continued increase in filler content may cause agglomeration and compromise the conductivity (Figure S1).[33] Next, a PC with a high dielectric constant and wide temperature window was used as a plasticizer, and optimal content in the GPE was evaluated. 0.75 ml PC can meet the requirements of ionic conductivity (Figure S2). Therefore, the following tests are done to the electrolyte with 0.075 g inert filler and 0.75 ml PC. Furthermore, commercial nanofillers with a size of 50 nm are used to avoid the effect of particle size (Figure S3). The filler-added GPE membranes exhibit a 3-dimensional network structure but with different pore sizes (Figure S4). The order of electrolyte ionic conductivity is filler-free > ZrO_2 > TiO_2 > Al_2O_3 > SiO_2 (Figure 1a and Figure S5), indicating that the effect of fillers on the conductivity of GPEs is different from that of polymer electrolytes.[34] As shown in Figure S6, there is no direct correlation between the crystallinity of the polymer and its ionic conductivity, suggesting that ion conduction does not occur along the polymer segments.[35]

Thermal stability was assessed by thermogravimetric analysis (TGA). As shown in Figure 1b, there are two weightless processes. Among them, the weightless around 180 ℃ corresponds to the volatilization of the PC solvent, and the PC content follows the same trend as the ionic conductivity. This finding confirms that the ion transport takes place in the solvent.[36] Another

weightless around 320 ℃ is due to the thermal decomposition of the polymer and the order of thermal stability is SiO_2 > Al_2O_3 > filler-free > TiO_2 > ZrO_2. The difference in thermal stability may originate from the different levels of interaction between the functional groups on the surface of the filler and the polymer.[37]

The addition of fillers also affects the mechanical strength of the electrolyte membrane (Figure 1c). The mechanical strength of the GPE with inert filler surpasses that of those without fillers due to the facile physical interaction between the surface of the inorganic nanoparticles and the polymer matrix, effectively acting as physical cross-linking points. Consequently, the mechanical strength of the system is improved. Among them, The PVDF-HFP-LiTFSI-PC-Al_2O_3 film shows the best mechanical strength because the intermolecular hydrogen bonding effect between Al_2O_3 nanofillers and PVDF-HFP makes the PVDF-HFP framework more mechanically robust.[38-40] Although the electrolyte membrane can withstand voltages greater than 4 V (Figure S7), interfacial side reactions still occur during the electrochemical reaction with the electrodes.[41] Furthermore, the interfacial properties were tested in NCM811//GPEs//Li using EIS spectroscopy. As shown in Figure 1d, the semicircle (R) represents the sum of the charge transfer resistance (R_{ct}) and the interfacial resistance (R_f).[42] The order of impedance in our study is Al_2O_3 < SiO_2 < TiO_2 < ZrO_2 < filler-free. The PVDF-HFP-LiTFSI-PC-Al_2O_3 film has a smaller impedance than other films before cycling, indicating good interface compatibility. This originates from the interaction between the hydroxyl groups on the surface of Al_2O_3 and the cathode.[43,44] Our results show that the ionic conductivity, thermal stability, mechanical strength, and interfacial properties have different trends. So the question is, what is the key factor to their electrochemical performance?

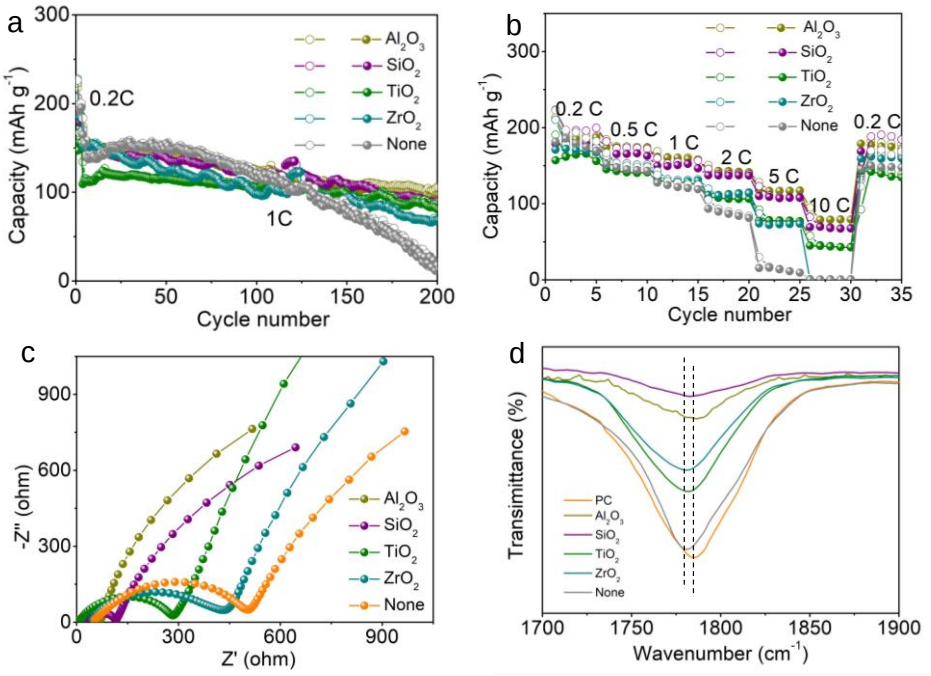

Figure 2. Electrochemical performance and post-cycle characterization. (a) Cycling performances, where 1 C= 180 mAh g^{-1}. (b) Rate performances. (c) EIS spectra after 5 cycles. (d) FTIR spectra of cathode after 5 cycles.

Electrochemical performances. As shown in Figures 2a and 2b, electrolyte membranes using different fillers show different cycling and rate performances when coupled with the NCM811 cathode (Figure S8). The Al_2O_3 film retains a capacity of 105.5 mAh g^{-1} after 200 cycles at a current density of 1 C, which is higher than that of SiO_2 (89.3 mAh g^{-1}), TiO_2 (84.6 mAh g^{-1}), ZrO_2 (68.3 mAh g^{-1}) and filler-free (17.6 mAh g^{-1}). Even at a high current density of 10 C, the capacity retention of the Al_2O_3 film is still 79.2 mAh g^{-1}, which is higher than that of SiO_2 (67.9 mAh g^{-1}), TiO_2 (44.6 mAh g^{-1}), ZrO_2 (0.7 mAh g^{-1}) and filler-free (0.6 mAh g^{-1}). This is consistent with literature findings that Al_2O_3 fillers the performs better compared to other fillers (Table S1). The capacity retention property is correlated with the interface impedance; a smaller

interface impedance corresponds to better rate performance and higher capacity. Next, EIS and FTIR characterizations after 5 cycles were performed for further verification. After 5 cycles, the interface resistance and charge transfer resistance become larger than those before the cycle, which is due to the formation of the interface film (Figure 2c).[45] The PVDF-HFP-LiTFSI-PC-Al_2O_3 film possesses a small R, which means fast charge and ion transfer at the interface. Compared with the uncycled electrolyte membranes (Figure S9), the C=O peak of PC in the cycled electrolyte membranes is all bule-shifted, except for that in Al_2O_3 which remains unchanged. Hence, the PC molecules decompose during the cycle and participate in the film formation, and these organic components give rise to the large impedance (Figure 2d), which confirms the effect of fillers on interfacial properties.[46] The abundant hydroxyl groups on the surface of Al_2O_3 make it most compatible with other cathode materials including $LiCoO_2$ and $LiFePO_4$ (Figure S10-12).

Interfacial property analysis. The interface structure after 5 cycles was analyzed by TEM. A visible interfacial layer appears on the surface of NCM811 with or without fillers in the electrolyte (Figure 3). The difference is that the interface film containing Al_2O_3 is thinner than the films without filler or that containing SiO_2, TiO_2, and ZrO_2 (Figure 3 and Figure S13). It is speculated that the fillers in the GPE change the interface properties between the cathode material and the GPE. Without fillers, the PC solvent molecules tend to undergo ring-opening polymerization under the action of the cathode, resulting in a thick and poor ionic conductivity film at the cathode interface.[47] When the filler is introduced, the functional groups on the surface of the filler interact with the cathode (see schematic in Figure 3), which inhibits the decomposition of PC by the cathode and changes the thickness and composition of the interfacial film (to be discussed below).

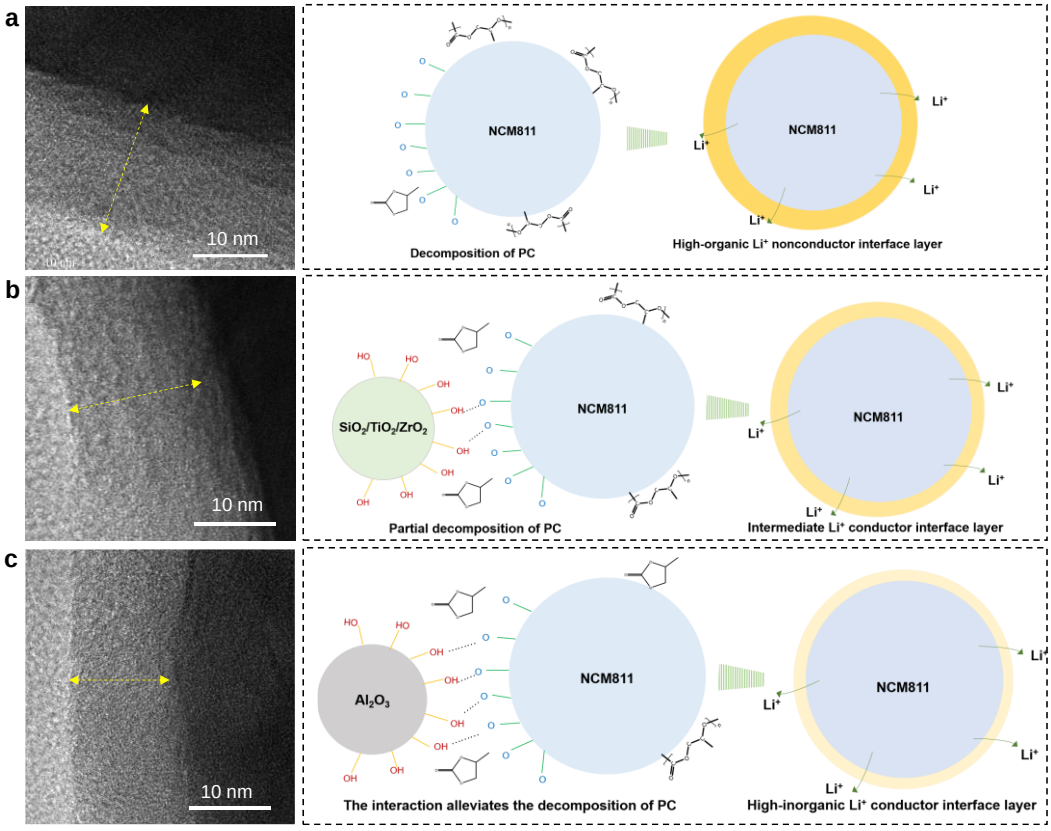

Figure 3. TEM images and schematic illustrations of the interfacial interactions. (a) Without inert fillers. (b) With TiO_2 inert fillers. (c) With Al_2O_3 inert fillers.

The interface composition after 5 cycles was further analyzed by XPS. As shown in Figure 4a, the peak around 289.5 eV belongs to the -CO_3 group adsorbed on the cathode surface after PC decomposition. In the absence of fillers, the -CO_3 content on the surface of the cathode is higher than those with inert fillers, which indicates that the addition of fillers can inhibit the decomposition of PC in GPE.[48] Next, the peak at 54.8 eV due to LiF is from is from the cathode electrolyte interfacial (CEI) film during cycling (Figure 4b). To further clarify the content of LiF, F 1s spectra were analyzed and the peaks at 684.2 and 687.2 eV due to Li-F and C-F bonds, respectively, are identified.[49] A relatively high LiF concentration is found in the PVDF-HFP-

LiTFSI-PC-Al_2O_3 film. In addition, the signals of Al 2p, Si 2p, and Zr 3d are also observed in the CEI films (Figure S14).

Based on the above analysis (Figures 3 and 4), we may draw the following conclusions about the interface: 1) PC decomposes during the electrochemical reaction and participates in the formation of the interfacial film. 2) The addition of nano-filler induces intermolecular interaction with the cathode and diminishes the decomposition of PC. Among these fillers, Al_2O_3 is the most favorable as the abundant hydroxyl functional groups on the surface of Al_2O_3 facilitate the formation of a high inorganic Li^+-conductive interface layer and accelerate the Li^+ transport at the interface. The construction of GPEs with high ion-conductivity interfaces is an important condition for achieving good battery performance.

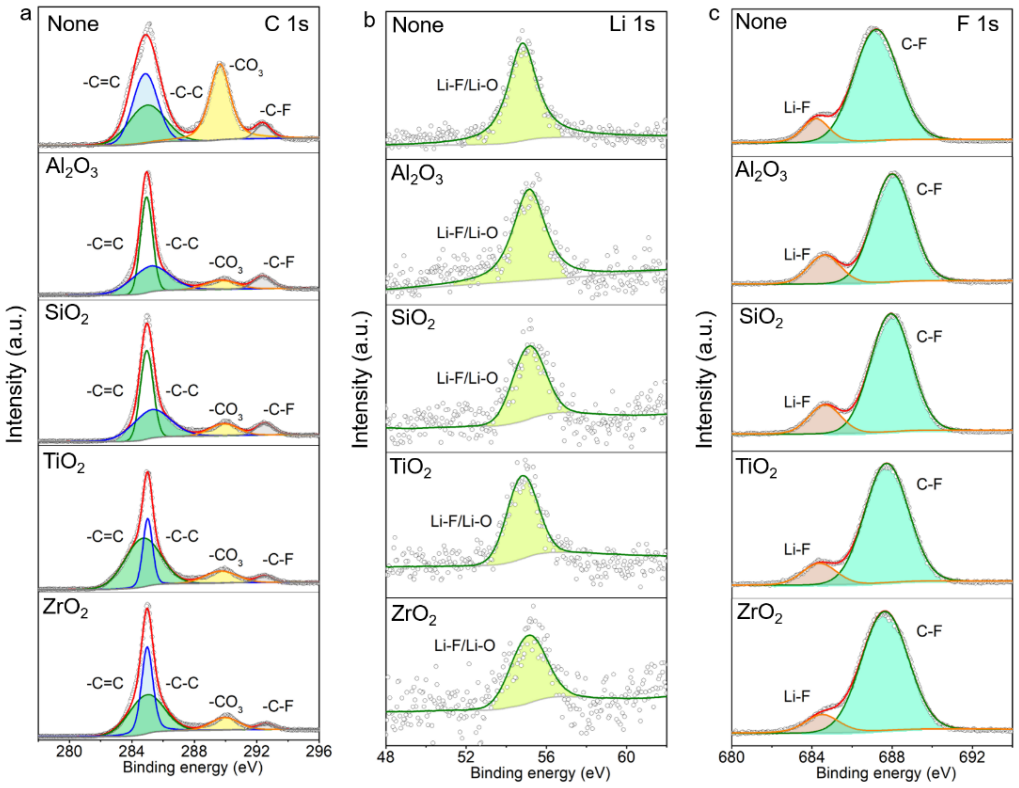

Figure 4. XPS spectra of GPEs with (Al_2O_3, SiO_2, TiO_2, ZrO_2) and without inert fillers. (a) C 1s, (b) Li 1s, (c) F 1s.

4. CONCLUSION

We have explored the main role of inert fillers in GPEs to understand how the battery performance is affected by adjusting the composition of the interfacial films. Among four types of common fillers (Al_2O_3, SiO_2, TiO_2, ZrO_2), Al_2O_3 contributes to the formation of a high ionic conductivity interfacial film by interacting with the cathode due to the abundant functional groups on the surface of Al_2O_3 particles. As a result, gel-polymer batteries containing Al_2O_3 exhibit the best electrochemical performance, and this conclusion is also valid even when extended to other cathode materials ($LiCoO_2$ and $LiFePO_4$). Hence, it is suggested that alumina can be used as both a coating material for the cathode and an electrolyte additive. The solvent in the GPE is a double-edged sword. While it maintains a high ionic conductivity and good interfacial contact, the interfacial side reactions generated by the catalytic decomposition of solvent are the main reason for the deterioration of performance. Therefore, it is a good strategy to control and stabilize the interface with fillers. This work provides a guide on how to improve the cycling stability of gel polymer batteries by choosing suitable inert fillers.

ASSOCIATED CONTENT

Supporting Information

The Supporting Information is available free of charge at https://pubs.acs.org/doi/.....

FTIR and XPS spectra, XRD patterns, SEM and TEM images, and more electrochemical characterizations including cycling performance, LSV, and EIS data (PDF)

AUTHOR INFORMATION

Corresponding Author

Hong Jin Fan - School of Physical and Mathematical Sciences, Nanyang Technological University, 21 Nanyang Link, Singapore 637371, Singapore

E-mail: fanhj@ntu.edu.sg

Authors

Jun Pan - School of Physical and Mathematical Sciences, Nanyang Technological University, Singapore 637371, Singapore

Pei Zhao - State Key Laboratory of High-Performance Ceramics and Superfine Microstructure, Shanghai Institute of Ceramics, Chinese Academy of Science, Shanghai 200050, China

Heliang Yao – State Key Laboratory of High-Performance Ceramics and Superfine Microstructure, Shanghai Institute of Ceramics, Chinese Academy of Science, Shanghai 200050, China

Lulu Hu - State Key Laboratory of High-Performance Ceramics and Superfine Microstructure, Shanghai Institute of Ceramics, Chinese Academy of Science, Shanghai 200050, China

Author Contributions

The manuscript was written through the contributions of all authors. All authors have given approval to the final version of the manuscript.

Notes

The authors declare no competing financial interest.

ACKNOWLEDGMENT

This work is financially supported from the Ministry of Education, Singapore, by its Academic Research Fund Tier 2 (MOE-T2EP50121-0006), and by the National Nature Science Foundation of China (No. 22209199).

REFERENCES

(1) Kang, K.; Meng, Y. S.; Breger, J.; Grey, C. P.; Ceser, G. Electrodes with High Power and High Capacity for Rechargeable Lithium Batteries. *Science* **2006**, *311*, 977-980.

(2) Harper, G.; Sommerville, R.; Kendrick, E.; Driscoll, L.; Slater, P.; Stolkin, R.; Walton, A.; Christensen, P.; Heidrich, O.; Lambert, S.; Abbott, A.; Ryder, K.; Gaines, L.; Anderson, P. Recycling Lithium-Ion Batteries from Electric Vehicles. *Nature* **2019**, *575*, 75-86.

(3) Sun, F.; He, X.; Jiang, X. Y.; Osenberg, M.; Li, J.; Zhou, D.; Dong, K.; Hilger, A.; Zhu, X. M.; Gao, R.; Liu, X. F.; Huang, K.; Ning, D.; Markötter, H.; Zhang, L.; Wilde, F.; Cao, Y. L.; Winter, M.; Manke, I. Advancing Knowledge of Electrochemically Generated Lithium Microstructure and Performance Decay of Lithium Ion Battery by Synchrotron X-ray Tomography. *Mater. Today* **2019**, *27*, 21-32.

(4) Zheng, Y.; Yao, Y. Z.; Ou, J. H.; Li, M.; Luo, D.; Dou, H. Z.; Li, Z. Q.; Amine, K.; Yu, A. P.; Chen, Z. W. A Review of Composite Solid-State Electrolytes for Lithium Batteries: Fundamentals, Key Materials and Advanced Structures. *Chem. Soc. Rev.* **2020**, *48*, 8790-8839.

(5) Cheng, Z. W.; Liu, T.; Zhao, B.; Shen, F.; Jin, H. Y.; Han, X. G. Recent Advances in Organic-Inorganic Composite Solid Electrolytes for All-Solid-State Lithium Batteries. *Energy Stor. Mater.* **2021**, *34*, 388-416.

(6) Pan, J.; Zhao, P.; Wang, N. N.; Huang, F. Q.; Dou, S. X. Research Progress on Stable Interfacial Constructions between Composite Polymer Electrolytes and Electrodes. *Energy Environ. Sci.* **2022**, *15*, 2753-2775.

(7) Song, J. Y.; Wang, Y. Y.; Wan, C. C. Review of Gel-Type Polymer Electrolytes for Lithium-Ion Batteries. *J. Power Sources* **1999**, *77*, 183-197.

(8) Long, L. Z.; Wang, S. J.; Xiao, M.; Meng, Y. Z. Polymer Electrolytes for Lithium Polymer Batteries. *J. Mater. Chem. A* **2016**, *4*, 10038-10069.

(9) Guo, Q. P.; Han, Y.; Wang, H.; Xiong, S. Z.; Sun, W. W.; Zheng, C. M.; Xie, K. Flame Retardant and Stable $Li_{1.5}Al_{0.5}Ge_{1.5}(PO_4)_3$-Supported Ionic Liquid Gel Polymer Electrolytes for High Safety Rechargeable Solid-State Lithium Metal Batteries. *J. Phys. Chem. C* **2018**, *122*, 10334-10342.

(10) Zhang, Q. Q.; Ding, F.; Sun, W. B.; Sang, L. Preparation of LAGP/P(VDF-HFP) Polymer Electrolytes for Li-Ion Batteries. *RSC Adv.* **2015**, *5*, 65395-65401.

(11) Guo, Q. P.; Han, Y.; Wang, H.; Xiong, S. Z.; Sun, W. W.; Zheng, C. M.; Xie, K. Novel Synergistic Coupling Composite Chelating Copolymer/LAGP Solid Electrolyte with Optimized Interface for Dendrite-Free Solid Li-Metal Battery. *Electrochim. Acta* **2019**, *296*, 693-700.

(12) Xu, D.; Su, J. M.; Jin, J.; Sun, C.; Ruan, Y. D.; Chen, C. H.; Wen, Z. Y.; In Situ Generated Fireproof Gel Polymer Electrolyte with $Li_{6.4}Ga_{0.2}La_3Zr_2O_{12}$ As Initiator and Ion-Conductive Filler. *Adv. Energy Mater.* **2019**, *9*, 1900611.

(13) Le, H. T. T.; Ngo, D. T.; Kalubarme, R. S.; Cao, G. Z.; Park, C. N.; Park, C. J. Composite Gel Polymer Electrolyte Based on Poly(vinylidene fluoride-hexafluoropropylene) (PVDF-HFP) with Modified Aluminum-Doped Lithium Lanthanum Titanate (A-LLTO) for High-Performance Lithium Rechargeable Batteries. *ACS Appl. Mater. Interfaces* **2016**, *8*, 20710-20719.

(14) Gao, H.; Huang, Y.; Zhang, Z.; Huang, J. X.; Li, C. $Li_{6.7}La_3Zr_{1.7}Ta_{0.15}Nb_{0.15}O_{12}$ Enhanced UV-Cured Poly(ethylene oxide)-Based Composite Gel Polymer Electrolytes for Lithium Metal Batteries. *Electrochim. Acta* **2020**, *360*, 137014.

(15) Huang, X. L.; Ma, X. G.; Wang, R.; Zhang, L.; Deng, Z. H. Combined Effect of Surface-Charged Latex Nanoparticle AHPS and Al_2O_3 Nano-Fillers on Electrochemical Performance of the Anionic Gel Polymer Electrolytes PVA/P(MA-co-AHPS). *Solid State Ion.* **2014**, *267*, 54-60.

(16) Redda, H. G.; Nikodimos, Y.; Su, W. N.; Chen, R. S.; Hagos, T. M.; Bezabh, H. K.; Weldeyohannes, H. H.; Hwang, B. J. The Surface Modification of Electrode Materials using Gel Polymer Electrolytes for Anode-Free Lithium Metal Batteries (AFLMB). *Mater. Today Energy* **2022**, *30*, 101141.

(17) Pan, X. N.; Yang, P. X.; Guo, Y.; Zhao, K. J.; Xi, B. J.; Lin, F.; Xiong, S. L. Electrochemical and Nanomechanical Properties of TiO_2 Ceramic Filler Li-Ion Composite Gel Polymer Electrolytes for Li Metal Batteries. *Adv. Mater. Interfaces* **2021**, *8*, 2100669.

(18) Wang, Z. Y.; Miao, C.; Zhang, Y.; Fang, R.; Yan, X. M.; Jiang, Y.; Tian, M. L.; Xiao, W. Preparation of Monodispersed ZrO_2 Nanoparticles and Their Applications in Poly[(vinylidene fluoride)-cohexafluoropropylene]-Based Composite Polymer Electrolytes. *PolymInt* **2018**, *67*, 894-900.

(19) Shen, Z. C.; Cheng, Y. F.; Sun, S. H.; Ke, X.; Liu, L. Y.; Shi, Z. C. The Critical Role of Inorganic Nanofillers in Solid Polymer Composite Electrolyte for Li^+ Transportation. *Carbon Energy* **2021**, *3*, 482-508.

(20) Yu, Q. J.; Jiang, K. C.; Yu, C. L.; Chen, X. J.; Zhang, C. J.; Yao, Y.; Jiang, B.; Long, H. J. Recent Progress of Composite Solid Polymer Electrolytes for All-Solid-State Lithium Metal Batteries. *Chin. Chem. Lett.* **2021**, *32*, 2659-2678.

(21) Huy, V. P. H.; So, S.; Hur, J. Inorganic Fillers in Composite Gel Polymer Electrolytes for High-Performance Lithium and Non-Lithium Polymer Batteries. *Nanomaterials* **2021**, *11*, 614.

(22) Wang, D. H.; Cai, D.; Zhong, Y.; Jiang, Z.; S. Zhang, Z.; Xia, X. H.; Wang, X. L.; Tu, J. P. A Three-Dimensional Electrospun $Li_{6.4}La_3Zr_{1.4}Ta_{0.6}O_{12}$-Poly (Vinylidene Fluoride-Hexafluoropropylene) Gel Polymer Electrolyte for Rechargeable Solid-State Lithium Ion Batteries. *Front. Chem.* **2021**, *9*, 751476.

(23) Bae, J.; Li, Y. T.; Zhang, J.; X. Zhou, Y.; Zhao, F.; Shi, Y.; Goodenough, J. B.; Yu, G. H. A 3D Nanostructured Hydrogel-Framework-Derived High-Performance Composite Polymer Lithium-Ion Electrolyte. *Angew. Chem. Int. Ed.* **2018**, *57*, 2096-2100.

(24) Wei, D.; Shen, W.; Xu, T.; Li, K.; Yang, L.; Zhou, Y.; Zhong, M.; Yang, F.; Xu, X.; Wang, Y.; Zheng, M.; Zhang, Y.; Li, Q.; Yong, Z.; Li, H.; Wang, Q. Ultra-Flexible and Foldable

Gel Polymer Lithium-Ion Batteries Enabling Scalable Production. *Mater. Today Energy* **2022**, *23*, 100889.

(25) Gu, L. M.; Zhang, M. Z.; He, J. L.; Ni, P. H. A Porous Cross-Linked Gel Polymer Electrolyte Separator for Lithium Ion Batteries Prepared by Using Zinc Oxide Nanoparticle As a Foaming Agent and Filler. *Electrochim. Acta* **2018**, *292*, 769-778.

(26) Yee, M.; An, K.; Nguyen, D. T.; Yun, H. W.; Park, J.; Suk, J.; Song, S. W. Confining Nonflammable Liquid in Solid Polymer Electrolyte to Enable Nickel-Rich Cathode-Based 4.2 V High-Energy Solid-State Lithium-Metal and Lithium-Ion Batteries. *Mater. Today Energy* **2022**, *24*, 100950.

(27) Zhao, M. K.; Zuo, X. X.; Wang, C. Y.; Xiao, X.; Liu, J. S.; Nan, J. M. Preparation and Performance of the Polyethylene-Supported Polyvinylidene Fluoride/Cellulose Acetate Butyrate/Nano-SiO_2 Particles Blended Gel Polymer Electrolyte. *Ionics* **2016**, *22*, 2123-2132.

(28) Yang, C. M.; Kim, H. S.; Na, B. K.; Kum, K. S.; Cho, B. W. Gel-Type Polymer Electrolytes with Different Types of Ceramic Fillers and Lithium Salts for Lithium-Ion Polymer Batteries. *J. Power Sources* **2006**, *156*, 574-580.

(29) Sun, Q. S.; Chen, X.; Xie, J.; Shen, C. H.; Jin, Y.; Huang, C.; Xu, X. W.; Tu, J.; Wang, B.; Zhu, T. J.; Zhao, X. B.; Cheng, J. P. Scale-Up Processing of a Safe Quasi-Solid-State Lithium Battery by Cathode-Supported Solid Electrolyte Coating. *Mater. Today Energy* **2021**, *21*, 100841.

(30) Wu, N.; Cao, Q.; Wang, X. Y.; Li, S.; Li, X. Y.; Deng, H. Y. In Situ Ceramic Fillers of Electrospun Thermoplastic Polyurethane/Poly(vinylidene fluoride) Based Gel Polymer Electrolytes for Li-Ion Batteries. *J. Power Sources* **2011**, *196*, 9751-9756.

(31) Chen, X. C.; Zhang, Y. M.; Merrill, L. C.; Soulen, C.; Lehmann, M. L.; Schaefer, J. L.; Du, Z. J.; Saito, T.; Dudney, N. J. Gel Composite Electrolyte-An Effective Way to Utilize Ceramic Fillers in Lithium Batteries. *J. Mater. Chem. A* **2021**, *9*, 6555-6566.

(32) Pan, J.; Wang, N. N.; Fan, H. J. Gel Polymer Electrolytes Design for Na-Ion Batteries. *Small Methods* **2022**, *6*, 2201032.

(33) Wu, M. J.; Liu, D.; Qu, D. Y.; Xie, Z. Z.; Li, J. S.; Lei, J. H.; Tang, H. L. 3D Coral-Like LLZO/PVDF Composite Electrolytes with Enhanced Ionic Conductivity and Mechanical Flexibility for Solid-State Lithium Batteries. *ACS Appl. Mater. Interfaces* **2020**, *12*, 52652-52659.

(34) Guo, J.; Hou, H. B.; Cheng, J. M.; Wang, C. D.; Wang, Q. G.; Sun, H. G.; Chen, X. Microporous Bayberry-Like Nano-Silica Fillers Enabling Superior Performance Gel Polymer Electrolyte for Lithium Metal Batteries. *J Mater Sci: Mater Electron* **2021**, *32*, 81-93.

(35) Lee, Y. S.; Lee, J. H.; Choi, J. A.; Yoon, W. Y.; Kim, D. W. Cycling Characteristics of Lithium Powder Polymer Batteries Assembled with Composite Gel Polymer Electrolytes and Lithium Powder Anode. *Adv. Funct. Mater.* **2013**, *23*, 1019-1027.

(36) Zhang, Z.; Huang, Y.; Li, C.; Li, X. Metal-Organic Framework-Supported Poly(ethylene oxide) Composite Gel Polymer Electrolytes for High-Performance Lithium/Sodium Metal Batteries. *ACS Appl. Mater. Interfaces* **2021**, *13*, 37262-37272.

(37) Jagadeesan, A.; Sasikumar, M.; Krishna, R. H.; Raja, N.; Gopalakrishna, D.; Vijayashree, S.; Sivakumar, P. High Electrochemical Performance of Nano TiO_2 Ceramic Filler Incorporated PVC-PEMA Composite Gel Polymer Electrolyte for Li-Ion Battery Applications. *Mater. Res. Express* **2019**, *6*, 105524.

(38) Jinisha, B.; Anilkumar, K. M.; Manoj, M.; Abnilash, A.; Pradeep, V. S.; Jayalekshmi, S. Poly (ethylene oxide) (PEO)-Based, Sodium Ion-Conducting, Solid Polymer Electrolyte Films, Dispersed with Al_2O_3 Filler, for Applications in Sodium Ion Cells. *Ionics* **2018**, *24*, 1675-1683.

(39) Mishra, K.; Arif, T.; Kumar, R.; Kumar, D. Effect of Al_2O_3 Nanoparticles on Ionic Conductivity of PVdF-HFP/PMMA Blend-Based Na^+-Ion Conducting Nanocomposite Gel Polymer Electrolyte. *J. Solid State Electrochem.* **2019**, *23*, 2401-2409.

(40) Xie, D. H.; Zhang, M.; Wu, Y.; Xiang, L.; Tang, Y. B. A Flexible Dual-Ion Battery Based on Sodium-Ion Quasi-Solid-State Electrolyte with Long Cycling Life. *Adv. Funct. Mater.* **2020**, *30*, 1906770.

(41) Zhou, Z.; Pei, X.; Zhang, T.; Wang, L. T.; Hong, J. H.; Lu, Y.; He, G. A Gel Polymer Electrolyte with 2D Filler-reinforced for Dendrite Suppression Li-Ion Batteries. *Electroanalysis* **2022**, *34*, 1-12.

(42) Zhao, L.; Huang, Y.; Liu, B.; Huang, Y. X.; Song, A. M.; Lin, Y. H.; Wang, M. S.; Li, X.; Cao, H. J. Gel Polymer Electrolyte Based on Polymethyl Methacrylate Matrix Composited with Methacrylisobutyl-polyhedral Oligomeric Silsesquioxane by Phase Inversion Method. *Electrochim. Acta* **2018**, *278*, 1-12.

(43) Croy, J. R.; O'Hanlon, D. C.; Sharifi-Asl, S.; Murphy, M.; Mane, A.; Lee, C. K.; Trask, S. E.; Shahbazian-Yassar, R.; Balasubramanian, M. Insights on the Stabilization of Nickel-Rich Cathode Surfaces: Evidence of Inherent Instabilities in the Presence of Conformal Coatings. *Chem. Mater.* **2019**, *31*, 3891-3899.

(44) Lee, J. H.; Amari, H.; Bahri, M.; Shen, Z. H.; Xu, C.; Ruff, Z.; Grey, C. P.; Ersen, O.; Aguadero, A.; Browning, N. D.; Mehdi, B. L. The Complex Role of Aluminium Contamination in Nickel-Rich Layered Oxide Cathodes for Lithium-Ion Batteries. *Batteries & Supercaps* **2021**, *4*, 1813-1820.

(45) Pan, J.; Zhang, Y. C.; Wang, J.; Bai, Z. C.; Cao, R. G.; Wang, N. N.; Dou, S. X.; Huang, F. Q. Quasi-Double-Layer Solid Electrolyte with Adjustable Interphases Enabling High-Voltage Solid-State Batteries. *Adv. Mater.* **2022**, *34*, 2107183.

(46) Wang, L.; Yan, J. W.; Zhang, R.; Li, Y. F.; Shen, W. Z.; Zhang, J. L.; Zhong, M.; Guo, S. W. Core-Shell PMIA@PVdF-HFP/Al_2O_3 Nanofiber Mats In Situ Coaxial Electrospun on $LiFePO_4$ Electrode as Matrices for Gel Electrolytes. *ACS Appl. Mater. Interfaces* **2021**, *13*, 9875-9884.

(47) Xu, S. Z.; Luo, G. F.; Jacobs, R.; Fang, S. Y.; Mahanthappa, M. K.; Hamers, R. J.; Morgan, D. Ab Initio Modeling of Electrolyte Molecule Ethylene Carbonate Decomposition Reaction on Li(Ni,Mn,Co)O_2 Cathode Surface. *ACS Appl. Mater. Interfaces* **2017**, *9*, 20545-20553.

(48) Chen, X. N.; Wang, X. H.; Fang, D. A Review on C1s XPS-Spectra for Some Kinds of Carbon Materials. *Fuller. Nanotub. Carbon Nanostructures* **2020**, *28*, 1048-1058.

(49) Pan, J.; Peng, H. L.; Yan, Y. H.; Bai, Y. Z.; Yang, J.; Wang, N. N.; Dou, S. X.; Huang, F. Q. Solid-state Batteries Designed with High Ion Conductive Composite Polymer Electrolyte and Silicon Anode. *Energy Stor. Mater.* **2021**, *43*, 165-171.

TOC Graphic

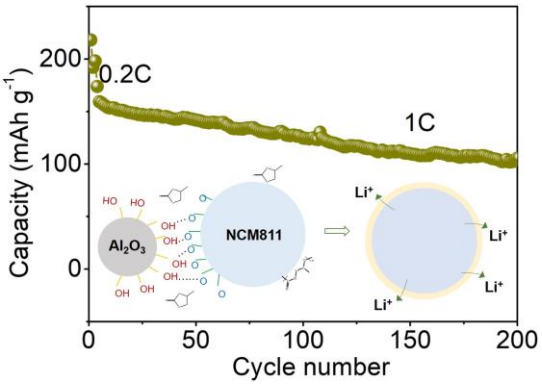

Through the intermolecular interaction between the functional groups on the filler surface and the cathode, it is a good strategy to improve the electrochemical performance by easing the decomposition of the organic solvent by the cathode material and forming a high-quality Li^+ conductor interface layer.